Available online at www.sciencedirect.com
SCIENCE DIRECT®
Bioorganic & Medicinal Chemistry 12 (2004) 4749–4759
Bioorganic & Medicinal Chemistry

Isoform-specific phosphoinositide 3-kinase inhibitors from an arylmorpholine scaffold

Zachary A. Knight,[a] Gary G. Chiang,[b] Peter J. Alaimo,[c] Denise M. Kenski,[a] Caroline B. Ho,[b] Kristin Coan,[a] Robert T. Abraham[b] and Kevan M. Shokat[c,d,*]

[a]*Program in Chemistry and Chemical Biology, University of California, San Francisco, CA 94143, USA*
[b]*Program in Signal Transduction Research, The Burnham Institute, La Jolla, CA 92037, USA*
[c]*Department of Cellular and Molecular Pharmacology, University of California, San Francisco, CA 94143, USA*
[d]*Department of Chemistry, University of California, Berkeley, CA 94720, USA*

Received 9 April 2004; accepted 10 May 2004
Available online 20 July 2004

Abstract—Phosphoinositide 3-kinases (PI3-Ks) are an ubiquitous class of signaling enzymes that regulate diverse cellular processes including growth, differentiation, and motility. Physiological roles of PI3-Ks have traditionally been assigned using two pharmacological inhibitors, LY294002 and wortmannin. Although these compounds are broadly specific for the PI3-K family, they show little selectivity among family members, and the development of isoform-specific inhibitors of these enzymes has been long anticipated. Herein, we prepare compounds from two classes of arylmorpholine PI3-K inhibitors and characterize their specificity against a comprehensive panel of targets within the PI3-K family. We identify multiplex inhibitors that potently inhibit distinct subsets of PI3-K isoforms, including the first selective inhibitor of p110β/p110δ (IC_{50} p110β = 0.13 μM, p110δ = 0.63 μM). We also identify trends that suggest certain PI3-K isoforms may be more sensitive to potent inhibition by arylmorpholines, thereby guiding future drug design based on this pharmacophore.

1. Introduction

Phosphatidylinositol 3-kinases are activated by a wide range of cell surface receptors to generate the lipid second messengers phosphatidylinositol 3,4-bisphosphate (PIP_2) and phosphatidylinositol 3,4,5-trisphosphate (PIP_3). In the appropriate cellular context, these two lipids can regulate a remarkably diverse array of physiological processes, including glucose homeostasis, cell growth, differentiation, and motility.[1] These distinct functions are carried out by a family of eight related PI3-Ks in vertebrates that possess unique substrate specificities, localization, and modes of regulation.[1] These include the class IA PI3-Ks (p110α, p110β, p110δ), which are activated by receptor tyrosine kinases, the class IB PI3-K (p110γ), which is activated by heterotrimeric G-proteins, and the class II PI3-Ks (PI3KC2α, PI3KC2β, PI3KC2γ) whose regulation remains poorly understood. Despite these known differences in upstream activation, the physiological roles of individual PI3-K isoforms remain largely unassigned, and dissecting the unique functions of members of this family is a major focus of ongoing research.[2]

In addition to sequence homology within their catalytic domain, PI3-Ks share sensitivity to two small molecule inhibitors, wortmannin and LY294002. Wortmannin is a fungal natural product that irreversibly inhibits PI3-Ks at low nanomolar concentrations,[3,4] whereas LY294002 is a synthetic chromone that reversibly inhibits most PI3-Ks at low micromolar concentrations.[5] Together, these two compounds have served as powerful probes for implicating PI3-Ks in a wide range of physiological processes, and much of our understanding of PI3-K action in cells derives from the use of these two reagents.

Although wortmannin and LY294002 are broadly active against the PI3-K family, they show little specificity among PI3-K family members. Since these compounds do not pharmacologically discriminate between PI3-K isoforms, comparatively little is known about the specific signaling functions of individual PI3-Ks. Knockout

Keywords: PI3-K; Inhibitor; Isoform; Phosphatidylinositol.
* Corresponding author. Tel.: +1-415-514-0472; fax: +1-415-514-0822; e-mail: shokat@cmp.ucsf.edu

0968-0896/$ - see front matter © 2004 Elsevier Ltd. All rights reserved.
doi:10.1016/j.bmc.2004.06.022

mice have defined essential roles for p110γ and p110δ in leukocyte function, including signaling from the B and T cell receptors[6,7] (p110δ) as well as chemotaxis of neutrophils and macrophages[8,9] (p110γ). Furthermore, microinjection of isoform-specific inhibitory antibodies has demonstrated that individual class I PI3-Ks can relay unique downstream signals following activation of a common upstream receptor. For example, colony-stimulating factor-1 treatment of macrophages induces DNA synthesis through p110α, whereas actin cytoskeleton rearrangement and cell migration require p110β and p110δ.[10] These studies suggest that PI3-K isoforms likely possess nonredundant functions downstream of the wide range of receptors that are known to activate PI3-Ks. In general, however, the systematic analysis of PI3-K isoform action in cells awaits the discovery of small molecule inhibitors that can selectively target PI3-K family members. For this reason, the development of isoform-specific inhibitors of PI3-Ks has been long anticipated.[2,11–13]

Recently, patent disclosures have described new inhibitors based on the LY294002 arylmorpholine pharmacophore,[11,12,14] although the detailed isoform selectivity of these compounds has not been reported. Since these compounds are potentially useful probes for PI3-K isoform activity in cells, we sought to determine their target specificity by characterizing their activity against a comprehensive panel of PI3-Ks. In this regard, a recent characterization of 28 common protein kinase inhibitors against a panel of 24 protein kinases has significantly challenged many preconceptions about the true selectivity of protein kinase inhibitors.[15] The analysis we report here identifies several compounds that inhibit distinct subsets of the PI3-K family, including the first selective inhibitors of the p110δ/p110β isoforms.

We also sought to explore the potential of the morpholino chromone scaffold as a starting point for PI3-K inhibitor optimization. LY294002 has been shown to be quite selective for lipid kinases relative to protein kinases[15] and to possess broad activity within the PI3-K family. Indeed, until very recently, LY294002 was the only reversible inhibitor that had been reported to target the PI3-K family—even though this compound was originally described 10 years ago.[5] Given the importance of PI3-Ks in signal transduction, it is remarkable that there has not been a single subsequent structure–activity study published investigating compounds of this class. Our comprehensive selectivity analysis of a panel of arylmorpholines identifies PI3-K isoforms that tend to be sensitive to this pharmacophore, as well as others that are more resistant. This information should prove useful in guiding future drug design based on this core structure.

2. Results

2.1. LY294002 analogs

Thrombogenix has disclosed a series of LY294002 analogs that differ in the substitution pattern of heteroatoms within the chromone core,[14] as well as through replacement of the phenyl group at the eight position of LY294002 with more extended aromatic substituents (Fig. 1). Comparison of the co-crystal structures of p110γ bound to LY294002[16] and ATP[17] suggests that the adenine ring of ATP and the morpholino-chromone core of LY294002 occupy essentially the same space in the interior of the ATP binding pocket, with both rings anchored by a hydrogen bond to the backbone amide of V882 (Fig. 1A). Likewise, the 8-phenyl moiety of LY294002 and the ribose sugar of ATP occupy a similar space at the entrance to the pocket and project outward toward solvent. To understand how LY294002 analogs with extended substitutents at C8 might interact differentially with PI3-K isoforms, we identified all of the residues in p110γ whose side chains possess a rotamer that can extend within 4 Å of either the adenine/LY294002 chromone

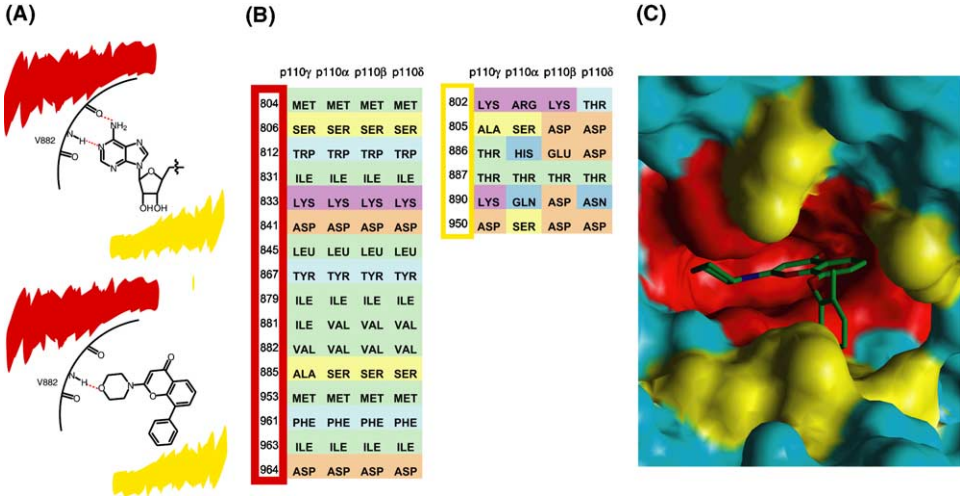

Figure 1. ATP binding site conservation among the class I PI3-Ks. (A) Schematic of the hydrogen bonds made by ATP (top) and LY294002 (bottom) in the active site of p110γ. Pocket interior (red) and entrance (yellow) are marked for reference. (B) Sequence of alignment residues in the interior (left) and exterior (right) of the ATP binding pocket. Residue coloring: hydrophobic aliphatic (green), hydrophobic aromatic (light blue), small (yellow), polar uncharged (dark blue), basic (purple), and acidic (orange). Residue number is for porcine p110γ. (C) Model of TGX115 bound to p110γ, based on the LY294002-p110γ co-crystal structure.[16]

core (Fig. 1, red) or the ATP ribose/8-phenyl of LY294002 (Fig. 1, yellow). This first set of residues defines the interior of the ATP binding pocket, while the second set mark the entrance to that pocket (Fig. 1C). We then aligned these residues with the corresponding residues from each of the class I PI3-Ks, and shaded them according to their physiochemical properties (hydrophobicity, size, and charge) (Fig. 1B). This alignment reveals that the interior of the ATP binding pocket is highly conserved within the class I PI3-Ks; the only differences are two conservative substitutions that distinguish p110γ from the class IA PI3-Ks (Fig. 1B, left). By contrast, the residues that line the entrance to the ATP binding pocket are divergent, with major differences between isoforms in their size and charge (Fig. 1B, right). LY294002 analogs with larger substituents at C8 would be expected to extend outside the ATP binding pocket and potentially make extensive contacts with these less conserved residues (Fig. 1C). This suggests that it may be possible for such extended analogs to target specific PI3-K isoforms, although it is not immediately apparent how to design compounds that would exploit these differences.

We initially prepared (Supplementary Schemes 1 and 2) and tested two compounds from this series (TGX115 and TGX126) as well as a synthetic intermediate lacking the aromatic substituent at C8 (TGX066) and compared these compounds to LY294002 and the related LY292223 (which lacks the C8 phenyl group). To obtain a detailed picture of the target specificity of these compounds, we determined IC_{50} values in vitro against a panel of 14 enzymes selected to span the most relevant targets for these molecules. These include seven mammalian PI3-Ks (p110α, p110β, p110δ, p110γ, PI3KC2α, PI3KC2β, and PI3KC2γ), four protein kinases in the PI3-K family (DNA-PK, ATM, ATR, mTOR), PI4-kinase β (a PI3-K family member reported to be weakly inhibited by LY294002[18]), casein kinase II (the only protein kinase family member known to be inhibited by LY294002[15]), and the unrelated serine-threonine kinase G-protein coupled receptor kinase 2 (GRK2). These 14 proteins include all of the known targets of LY294002 and most of the proteins that contain sequence homology to the PI3-K catalytic domain. To facilitate comparison of IC_{50} values across kinases with different substrate affinities, all assays were carried out in the presence of 100 μM ATP.

As has been previously reported, LY29002 exhibits a very broad specificity profile, inhibiting the class I PI3-Ks, PI3KC2β, PI3KC2γ, mTOR, casein kinase 2, and DNA-PK all with IC_{50} values in the low micromolar range. Within the class I PI3-Ks, LY294002 exhibits a maximum of approximately 10-fold selectivity between any two isoforms, with p110β being most sensitive (2.9 μM) and p110γ the least sensitive (38 μM). Interestingly, LY294002 did not show activity at 100 μM against the PI3-K related protein kinases ATM and ATR. Although we are not aware of any reports that LY294002 inhibits these two enzymes at micromolar concentrations,[19] the effects of LY294002 treatment of cells has been interpreted to imply a requirement for ATM or ATR kinase activity in several studies.[20,21]

In contrast to LY294002, TGX115 and TGX126 were significantly more potent and selective. Surprisingly, we find that TGX115 inhibits p110β and p110δ at nanomolar concentrations, but p110α and p110γ only at concentrations more than 100-fold higher (Fig. 2). TGX126 showed a more modest specificity profile, although this compound was still ~50-fold more potent against p110β/p110δ than against p110α/p110γ. Against the other 10 enzymes in this panel, TGX115 and TGX126 showed significant activity only against DNA-PK, with high nanomolar IC_{50} values. Thus, within the lipid kinases, these two compounds represent the first selective inhibitors of the p110β/p110δ isoforms. By contrast, the unsubstituted analogs TGX066 and LY292223 were significantly less potent against all PI3-Ks, although they retained strong activity against DNA-PK (Fig. 2). This suggests that presence of an aromatic substituent at C8 plays an essential role in achieving binding affinity for PI3-Ks, but may be dispensable for DNA-PK inhibition.

On the basis of this initial data, seven additional compounds were prepared by palladium catalyzed coupling of different aromatic substituents to TGX066 (Supplementary Scheme 1) to explore the chemical space surrounding TGX115 and TGX126. These compounds, termed morpholino chromone analogs 49–55 (MCA049–MCA055), all contain the pyrimidone heterocycle scaffold of TGX126 and differ in their aromatic substitution at the position analogous to C8 in LY294002. They include compounds that substitute the pyrimidone core with anilines (MCA50–MCA52, MCA54), benzylamines (MCA53 and MCA55), and a biaryl linkage (MCA49) that mimics LY294002 in this new scaffold, and were prepared.

The specificity profile of these compounds was determined, and several structure–activity trends were identified (Fig. 2). Compounds containing a benzylamine substitution to the pyrimidone core exhibit potent activity against the class IA PI3-Ks p110α/β/δ ($IC_{50} = 0.1-2\,\mu M$), but display comparatively less activity against the class IB PI3-K p110γ ($IC_{50} = 25-100\,\mu M$). Compared to the closely related TGX126, these methyl-substituted compounds possess modestly enhanced activity toward p110α and diminished activity against p110γ. MCA55 showed the largest selectivity between p110α and p110γ of any compound in our panel (~50-fold) and this compound can be regarded as a multiplex inhibitor of the growth factor regulated class IA PI3-Ks with little activity against the G-protein regulated class IB enzyme, p110γ.

In contrast, compounds containing an aniline substitution on the pyrimidone scaffold all showed a 10–100-fold loss of activity against the PI3-K isoforms p110δ and p110β relative to the parent compounds TGX115 and TGX126, while retaining potent DNA-PK inhibition. This trend includes MCA51, a compound that is isosteric to TGX115 within the pyrimidone scaffold. Compared to TGX115, this compound is ~20-fold less potent against p110δ/p110β and ~10-fold more potent against DNA-PK. This effect appears to be a

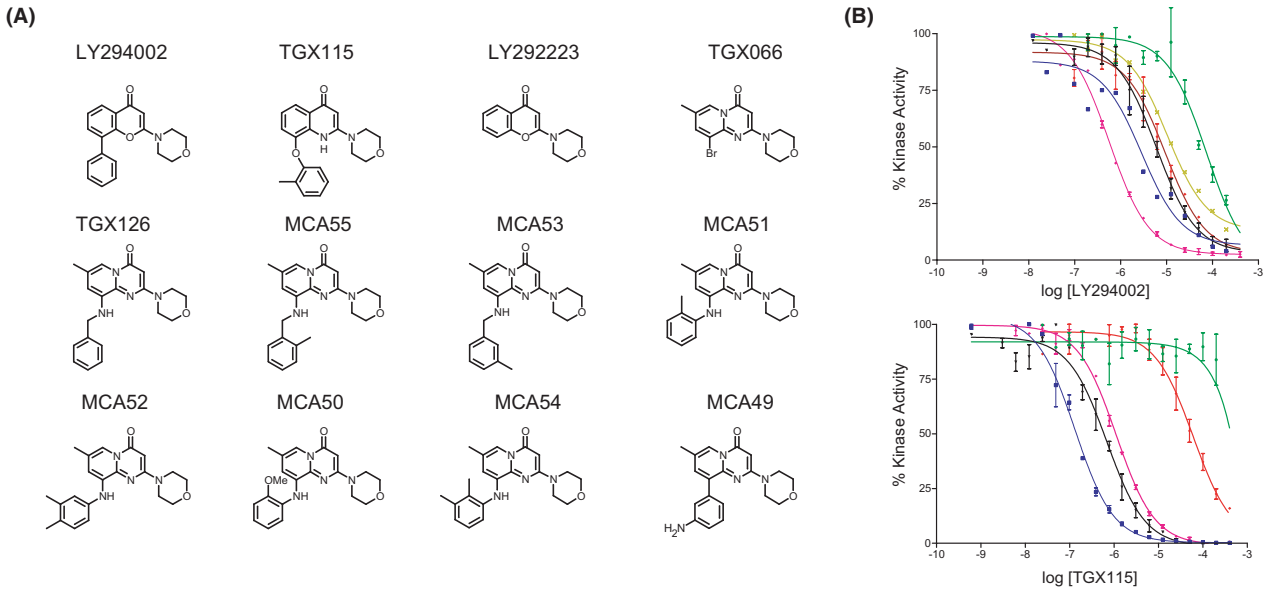

(C)

	p110α	p110β	p110δ	p110γ	PIKC2α	PIKC2β	PIKC2γ	PI4Kβ	DNA-PK	ATM	ATR	mTOR	CK2	GRK2
TGX115	61	0.13	0.63	~100	>100	~50	~100	>100	1.2	>100	>100	>100	>100	>100
TGX126	8.1	0.16	0.15	~10	ND	ND	ND	>100	0.28	ND	ND	ND	>100	>100
TGX066	58	9.9	8.5	>100	ND	ND	ND	>100	1.3	>100	ND	>100	>100	>100
MCA49	14	18	6.9	38	ND	>100	ND	ND	7.1	ND	ND	ND	ND	ND
MCA50	~50	~20	~10	>100	>100	>100	>100	>100	0.19	>100	ND	>100	>100	>100
MCA51	~9	3.3	3.8	>100	>100	>100	~50	>100	0.15	>100	ND	>100	>100	>100
MCA52	~10	14	~5	>100	>100	ND	~50	>100	0.55	>100	ND	>100	>100	>100
MCA53	1.8	0.99	0.39	~25	>100	~10	>100	>100	0.38	>100	ND	>100	>100	>100
MCA54	6.2	3.5	3.3	~100	>100	ND	~50	>100	0.36	>100	ND	>100	>100	>100
MCA55	1.1	0.11	0.87	~100	>100	2.8	~50	>100	0.27	>100	>100	>100	>100	>100
LY292223	45	7.5	13	~100	ND	~100	~20	>100	0.42	ND	ND	ND	>100	>100
LY294002	9.3	2.9	6.0	38	~100	5.7	40	~100	0.66	>100	>100	8.9	12.2	>100

Figure 2. IC_{50} values of LY294002 analogs against protein and lipid kinases. (A) Structures of LY294002 analogs. (B) Dose response curves for LY294002 (top) and TGX115 (bottom) against different PI3-K family members. DNA-PK (purple), p110α (red), p110β (blue), p110γ (green), p110δ (black), and CK2 (yellow). (C) IC_{50} values (μM) measured in the presence of 100 μM ATP.

consequence of the aniline substitution, rather than the pyrimidone core itself, because TGX126 and related compounds containing a benzylamine substitution remain highly potent against p110δ/p110β. This suggests that very subtle changes to the aromatic substituent can significantly shift inhibitor specificity among PI3-K family members. Indeed, we find that several anilino-pyrimidones inhibit DNA-PK at nanomolar concentrations and display significant selectivity (10–100-fold) relative to all other members of the PI3-K family. These compounds may prove useful as selective inhibitors of DNA-PK, or as lead structures for the development of more highly specific compounds.

2.2. Arylmorpholine DNA-PK inhibitors

ICOS has recently disclosed a set of arylmorpholines[22,23] that are potent inhibitors of DNA-PK (Fig. 3). These compounds are trisubstituted benzene derivatives with hydroxy and carbonyl moieties *meta* and *para* to the morpholine ring, respectively. As these molecules are structurally reminiscent of LY294002, we prepared a small set of eight arylmorpholines (Supplementary Scheme 3) and determined their specificity profile against our enzyme panel.

We find that IC60211 and IC86621 are high nanomolar inhibitors of DNA-PK, with IC_{50} values against class I PI3-Ks in the low to mid-micromolar range, consistent with an earlier report.[22] In this regard, these compounds exhibit a specificity profile that mirrors LY294002, with modestly enhanced DNA-PK activity (1.5–5-fold). Nonetheless, we find that these compounds are more selective than LY294002 in that they show no activity against the secondary targets mTOR, casein kinase II or any of the class II PI3-Ks. Thus, within the lipid kinases, this structural class is selective for the class I PI3-Ks. Arylmorpholine analog 37 (AMA37) is the most DNA-PK selective of these compounds, with ~10-fold specificity relative to p110β and ~100-fold specificity relative to the other class I PI3Ks. This potency and selectivity is comparable to the most DNA-PK selective compounds identified from our panel of anilino pyrimidones.

We tested a series of analogs of these compounds to probe the requirements for DNA-PK inhibition, and confirm that both the hydrogen bond acceptor at the 1-position and the donor at the 2-position are required for potent DNA-PK inhibition (Fig. 3). For example, AMA57, which differs from AMA37 by the substitution

(A)

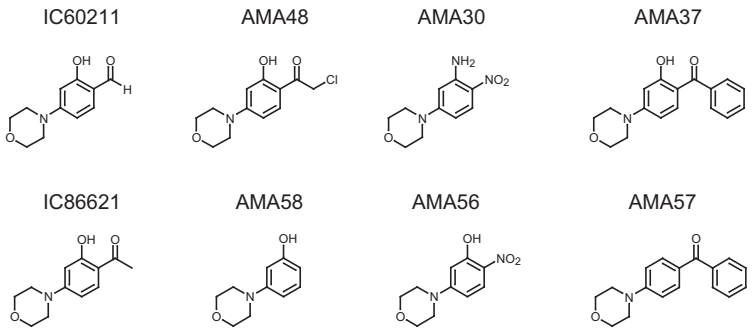

(B)

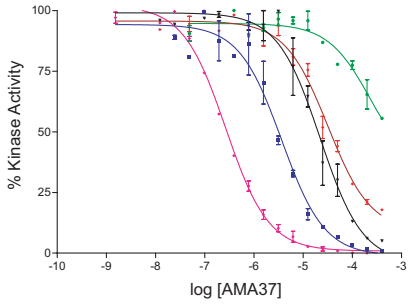

(C)

	p110α	p110β	p110δ	p110γ	PIKC2α	PIKC2β	PIKC2γ	PI4Kβ	DNA-PK	ATM	ATR	mTOR	CK2	GRK2
AMA30	~100	23	24	~100	ND	ND	ND	>100	2.3	>100	ND	>100	>100	>100
IC60211	~10	2.8	5.1	37	>100	>200	~50	>100	0.43	>100	ND	>100	>100	>100
IC86621	16	0.99	3.8	10	ND	~200	>100	>100	0.17	>100	ND	>100	>100	>100
AMA37	32	3.7	22	~100	>100	~200	~50	>100	0.27	>100	>100	>100	>100	>100
AMA48	30	ND	4.8	~70	ND	ND	ND	>100	1.1	>100	ND	>100	>100	>100
AMA56	ND	ND	ND	ND	ND	ND	ND	ND	1.2	ND	ND	ND	ND	ND
AMA57	ND	ND	ND	ND	ND	ND	ND	ND	14.7	ND	ND	ND	ND	ND
AMA58	ND	ND	ND	ND	ND	ND	ND	ND	~100	ND	ND	ND	ND	ND

Figure 3. IC_{50} values of arylmorpholines against protein and lipid kinases. (A) Structures of arylmorpholine analogs. (B) Dose response curves for AMA37 against different PI3-K family members (color coded as in Fig. 2). (C) IC_{50} values (μM) measured in the presence of 100 μM ATP.

of a hydrogen for the 2-hydroxyl, is ~80-fold less potent, whereas AMA58, which differs from IC60211 potent. However, the specific identity of hydrogen bond donor and acceptor is not a requirement for potent DNA-PK inhibition. For example, AMA56, which differs from IC60211 by the replacement of the aldehyde with a nitro group, is only ~3-fold less potent. Likewise, AMA30, which differs from AMA56 by the further substitution of the 2-hydroxyl group with an amine, is only ~2-fold less potent.

3. Discussion

We have measured the activity of a panel of compounds that share the arylmorpholine pharmacophore first identified in LY294002 against a comprehensive set of targets within the PI3-K family. Analysis of this data suggests several trends in selectivity among different PI3-K family members. First, while we confirm that LY294002 inhibits three protein kinases at low micromolar concentrations (DNA-PK, mTOR, CK2), we find that two of these kinases (mTOR and CK2) are resistant to all other arylmorpholines in our panel. DNA-PK, by contrast, is potently inhibited by almost every compound tested, and shows very broad SAR with respect different analogs in the same series. In part, we believe these differences reflect the fact that DNA-PK binds with high affinity to the core arylmorpholine pharmacophore, whereas the other protein kinases (and to a lesser extent, the PI3-Ks) require more extensive interactions with other regions of the molecule for high affinity binding. Consistent with this view, the most structurally simple compounds in our panel (TGX066, LY292223, and IC60211) all exhibit potent inhibition of DNA-PK, even though their PI3-K activity is significantly reduced compared to more substituted analogs. Moreover, a third class of DNA-PK inhibitors based on a limited arylmorpholine scaffold have recently been reported,[24] suggesting that diverse compounds containing this core structure can exhibit potent and selective DNA-PK inhibition.

Selectivity trends were also observed within the class I PI3-Ks. To visualize these differences, we plotted the IC_{50} values of all of the compounds for inhibition of p110β (*x*-axis) against the IC_{50} values for inhibition of the other class I PI3-Ks and DNA-PK (*y*-axis), such that each data point represents the intersection of IC_{50} values for the same compound against two different enzymes (Fig. 4). In this representation, compounds that lie along

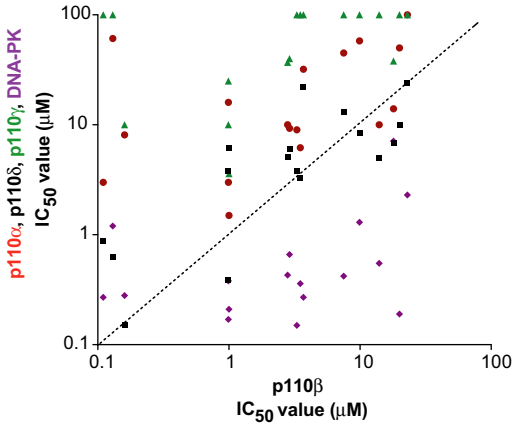

Figure 4. Correlation plot for inhibition of different PI3-K isoforms. IC_{50} values (μM) for p110β (*x*-axis) plotted against IC_{50} values for DNA-PK (purple), p110α (red), p110γ (green), and p110δ (black).

the diagonal show equipotent inhibition of p110β and the second kinase, whereas those that lie above or below the diagonal are more or less potent, respectively, against the second enzyme than p110β. Virtually all of the DNA-PK IC_{50} values (purple) occupy the lower section of the plot, reflecting the fact that DNA-PK is more sensitive to arylmorpholines than the class I PI3Ks. p110δ IC_{50} values (black) cluster around the diagonal as few compounds within this series show differential activity against p110δ and p110β, whereas p110α (red) tends to be inhibited less potently. p110γ (green) was unexpectedly resistant to inhibition by a large number of arylmorpholines, although this insensitivity is consistent with p110γ's underlying poor sensitivity to LY294002 relative to the other class I isoforms.

While we have not been able to rationalize these differences in inhibitor sensitivity in terms of specific residues that differ between PI3-K isoforms, several observations are consistent with these IC_{50} trends. First, the similarity in the sensitivity of p110δ and p110β to diverse compounds is likely a reflection of the fact that these two kinases are more closely related in primary sequence than any other members of the PI3-K family. For this reason, it may be challenging to find analogs of potent p110β/p110δ inhibitors such as TGX115 containing the arylmorpholine core that can distinguish between these two isoforms. Second, we find that the overall trend in inhibitor sensitivity among these targets (p110γ < p110α < p110β, p110δ < DNA-PK) roughly mirrors the K_M for ATP of these proteins. That is, we have found that p110γ has the lowest K_M for ATP among these enzymes (7.4 μM), whereas DNA-PK has the highest (192 μM), and the class IA PI3-Ks exhibit intermediate values. While this alone cannot explain the potency and isoform selectivity of compounds such as TGX115, it does suggest that smaller differences between the class I isoforms (e.g., as observed for LY294002) likely reflect differential competition from ATP substrate between isoforms. This suggests that the PI3-K family members for which selective inhibitors have been identified to date (DNA-PK, and, to a lesser extent, p110β and p110δ) may be inherently easier to target with ATP competitive small molecules than other isoforms.

It has long been anticipated that the development of isoform-specific PI3-K inhibitors would make it possible to dissect the unique contributions of individual PI3-K isoforms in well-characterized signaling pathways.[2,11–13] Recently, Sadhu et al. described the first isoform selective PI3-K inhibitor,[25] IC87114, which targets p110δ, and this compound has found rapid use in identifying essential roles for p110δ in chemotaxis and inflammatory responses of neutrophils,[25–27] spontaneous tone of arteries[28] and EGF driven migration of cancer cell lines.[29] TGX115, when used either in conjunction with IC87114 or in cells that do not express p110δ, should prove equally effective in elucidating physiological roles for p110β, and we have begun to use this compound to explore p110β mediated signaling in several systems (Z.A.K. and K.M.S., unpublished results). As other mutliplex inhibitors we describe in this report also possess activity against unique combinations of PI3-K family members (Fig. 5), it may be possible to use these compounds in combination in order to interrogate additional PI3-K isoforms. In this way, we envision a route to begin to pharmacologically dissect the distinct contributions of members of this important family of signaling enzymes.

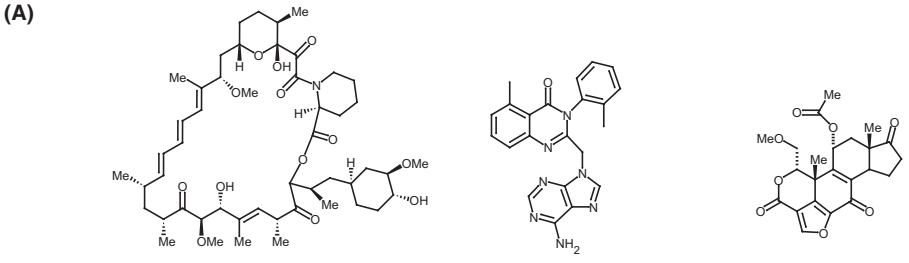

(B)

	p110α	p110β	p110δ	p110γ	C2α	C2β	C2γ	DPK	ATM	ATR	TOR
Wortmannin (mid μM)	X	X	X	X	X	X	X	X	X		X
Wortmannin (mid nM)	X	X	X	X		X	X				
LY294002	X	X	X	X		X	X	X			X
IC60211	X	X	X	X				X			
MCA055	X	X	X			X		X			
TGX115		X	X					X			
IC87114, others			X								
AMA037, others								X			
Rapamycin											X

Figure 5. Spectrum of characterized PI3-K inhibitor selectivities. (A) Structures of reported inhibitors of PI3-K family members. (B) Selectivity profile of well-characterized PI3-K inhibitors. Data for wortmannin, IC87114, and rapamycin is drawn from published reports. Compounds characterized in this study are highlighted in red.

4. Experimental

4.1. Lipid kinase expression

Epitope tagged p110α, p110β, p110δ, PI3KC2α, PI3KC2β, and PI3KC2γ were expressed by transient transfection of cos-1 cells. Cells were lyzed in lysis buffer (50 mM Tris (pH 7.4), 300 mM NaCl, 5 mM EDTA, 0.02% NaN_3, 1% Triton X-100, and protease inhibitors) and the kinase immunoprecipitated with the appropriate antibody-protein G complex. Immunoprecipitates were washed twice with buffer A (PBS, 1 mM EDTA, 1% Triton X-100), twice with buffer B (100 mM Tris (pH 7.4), 500 mM LiCl, 1 mM EDTA), and twice with buffer C (50 mM Tris (pH 7.4), 100 mM NaCl). GST-PI4Kβ was expressed in BL21 *E. coli* and purified by glutathione chromatography essentially as described.[18] Recombinant p110γ was obtained from Sigma. In control experiments, no differences in inhibitor sensitivity were observed between p110α immunoprecipitated from cos-1 cells and protein expressed in Sf9 cells using a baculovirus system.

4.2. Lipid kinase assays

All kinase assays were conducted at a final concentration of 100 μM ATP and 2% DMSO. PI3-K and PI4-K assays were carried out essentially as described.[18] Briefly, a reaction mixture was prepared containing kinase, inhibitor, buffer (25 mM HEPES (pH 7.4), 10 mM $MgCl_2$), and freshly sonicated phosphatidylinositol (200 μg/mL). Reactions were initiated by the addition of ATP containing 10 μCi of γ-^{32}P-ATP to a final concentration 100 μM. Reactions were incubated 15 min at rt and then terminated by the addition of 105 μL 1 N HCl followed by 160 μL $CHCl_3$–MeOH (1:1). The biphasic mixture was then vortexed, briefly centrifuged, and the organic phase transferred to a new tube using a gel loading pipette tip precoated with $CHCl_3$. This extract was spotted on TLC plates and developed for 3–4 h in a 65:35 solution of *n*-propanol–2 M AcOH. The TLC plates were then dried and quantitated using a PhosphorImager (Molecular Dynamics). For each compound, kinase activity was measured at 12–15 inhibitor concentrations representing twofold dilutions from the highest concentration tested (typically, 200 μM). For compounds showing significant activity, IC_{50} determinations were repeated two to six times, and the reported value is the average of these independent measurements.

4.3. Protein kinase expression

HA-ATM, FLAG-ATR, and AU-1 mTOR were expressed by transient transfection of HEK293 cells. The cells were lyzed in lysis buffer (50 mM Tris–Cl (pH 7.4), 100 mM NaCl, 50 mM β-glycerophosphate, 10% glycerol (w/v), 1% Tween-20, 1 mM EDTA, 25 mM NaF, and protease inhibitors), and lysates were subjected to immunoprecipitation with the appropriate epitope-tag antibody. Immune complexes were collected on rabbit anti-mouse Sepharose (Sigma) and washed three times in lysis buffer, once in high salt buffer (100 mM Tris–Cl (pH 7.4), 500 mM LiCl), and once in kinase wash buffer (10 mM HEPES (pH 7.4), 50 mM NaCl, 50 mM β-glycerophosphate, 10% glycerol). N-terminal His6-tagged GRK2 was expressed in Sf9 insect cells and purified using Ni-NTA beads (Qiagen) as described.[30] Casein kinase 2 was obtained from Upstate Biotechnology, and DNA-PK was obtained from Promega.

4.4. Protein kinase assays

ATM, ATR, and mTOR immunoprecipitates were resuspended in kinase assay buffer (10 mM HEPES (pH 7.4), 50 mM NaCl, 50 mM β-glycerophosphate, 10% glycerol, 10 mM $MnCl_2$, 1 mM DTT) and incubated with inhibitor for 30 min prior to the kinase reaction. Kinase reactions were initiated by the addition of 100 μM ATP, 10 μCi (γ-^{32}P)-ATP and 1 μg of either a GST-p70S6K fragment (amino acids 332–414) for mTOR, or 1 μg of a GST-p53 fragment (amino acids 1–70) for ATM or ATR. Reactions were incubated at 30 °C for 20 min and terminated by the addition of 2× SDS-PAGE sample buffer. Samples were resolved by SDS-PAGE and transferred to PVDF membranes. The portion of the membrane containing the ^{32}P-labeled substrate was quantitated by PhosphorImager, while the portion of the membrane containing ATM, ATR, or mTOR was subjected to Western blotting with anti-HA, anti-FLAG, or anti-AU1 antibody, respectively.

The amount of ^{32}P incorporation in the substrate was normalized to the amount of ATM or mTOR present. GRK2 assays were carried out using tubulin as substrate in 20 mM HEPES, pH 7.4, 2 mM EDTA, 10 mM $MgCl_2$ containing 100 μM ATP essentially as described.[30] DNA-PK assays were carried out using the DNA-PK assay system (Promega) as directed by the manufacturer. Casein kinase 2 assays were carried out using the casein kinase 2 assay kit (Upstate Biotechnology) as directed by the manufacturer.

4.5. Synthesis

4.5.1. General. The following reagents were obtained commercially: 2-amino-2′-methyldiphenyl ether (TCI America), 3-morpholinophenol (Avacado Research), 4-morpholinobenzophenone (Sigma), 5-morpholino-2-nitrophenol (Alfa Aesar), LY294002 (Calbiochem), and MnO_2 and $PdCl_2$ (dppf) (Strem Chemicals). All other reagents were from Aldrich, were of the highest grade commercially available, and were used as supplied by the manufacturer without further purification. Reversed phase high performance liquid chromatography (RP-HPLC) was performed on a Ranin SD-200 solvent delivery system equipped with a Zorbax 300-SB C18 column using a MeCN/H_2O/0.1% TFA gradient (0–100%) as the mobile phase.

4.5.2. 5-(Bis-methylsulfanyl-methylene)-2,2-dimethyl-(1,3)dioxane-4, 6-dione (1). Triethylamine (9.6 mL, 69 mmol) and CS_2 (2.05 mL, 34.7 mmol) were added consecutively to a stirred solution of Meldrum's acid (5.0 g, 35 mmol) in DMSO (50 mL) at rt.[31] After 1 h, the reaction was cooled on ice, MeI (4.3 mL, 69 mmol) was added, and the reaction was allowed to proceed

overnight at rt. After 18 h, the reaction was terminated by adding ice water, and the precipitate was chromatographed on silica gel (50% EtOAc/hexanes) to yield 1.962 g (23%) of a yellow solid. ^{1}H NMR (400 MHz, $CDCl_3$) δ 2.45 (6H, s), 1.53 (6H, s).

4.5.3. 2,2-Dimethyl-5-(1-methylsulfanyl-2-(2-o-tolyloxy-phenyl)-ethylidene)-(1,3)dioxane-4,6-dione (2). 2-Amino-2′-methyldiphenyl ether (802 mg, 4.03 mmol) was added to a solution of **2** (1.0 g, 4.0 mmol) in EtOH (9 mL) and stirred at reflux for 9 h essentially as described.[14,32] When the reaction was complete, the solvent was removed in vacuo and the product chromatographed twice on silica (10% EtOAc/hexanes followed by 50% EtOAc/hexanes) to yield 1.54 g (95.8%). ^{1}H NMR (400 MHz, $CDCl_3$) δ 7.39 (1H, d, J = 8 Hz), 7.00–7.24 (5H, m), 6.78–6.81 (2H, m), 5.24 (1H, s), 2.27 (3H, s), 2.21 (3H, s), 1.66 (6H, s); ^{13}C NMR (100 MHz, $CDCl_3$) δ 178.5, 153.8, 151.3, 131.8, 129.8, 129.5, 128.0, 127.7, 127.3, 124.7, 123.1, 118.9, 117.9, 117.1, 103.2, 86.8, 26.5, 19.0, 16.3.

4.5.4. 2-Morpholin-4-yl-8-o-tolyloxy-1H-quinolin-4-one (TGX115). Morpholine (0.44 mL, 5.0 mmol) was added to a solution of **2** (900 mg, 2.25 mmol) in THF (12 mL).[14] The reaction was heated to reflux for 24 h. After cooling to rt, the solvent was removed in vacuo, the solid washed with Et_2O, and then dissolved in Ph_2O (10 mL). The reaction was heated to 265 °C for 15 min, and then cooled to rt. The product was purified by chromatography on silica gel twice (50% EtOAc/hexanes followed by 10% MeOH/EtOAc) to yield 227 mg (33%) of a white solid. ^{1}H NMR (400 MHz, $CDCl_3$) δ 8.51 (1H, s), 7.88 (1H, d, J = 8 Hz), 7.11–7.27 (3H, m), 7.05 (1H, t, J = 16 Hz), 6.94 (1H, d, J = 8 Hz), 6.67 (1H, d, J = 8 Hz), 5.73 (1H, s), 3.81 (4H, s), 3.29 (4H, t, J = 4 Hz), 2.18 (3H, s); ^{13}C NMR (100 MHz, DMSO-d_6) δ 161.6, 157.7, 157.0, 149.7, 140.9, 130.6, 126.8, 126.6, 121.7, 120.6, 119.6, 118.9, 117.6, 115.9, 91.1, 65.8, 44.8, 16.1; HR-EI MS $(M)^+$ m/z calcd for $C_{20}H_{20}N_2O_3$ 336.1474, found 336.1457.

4.5.5. 9-Bromo-2-hydroxy-7-methyl-pyrido(1,2-a)pyrimidin-4-one (3). A stirred solution of 2-amino-3-bromo-5-methylpyridine (9.85 g, 52.7 mmol) in diethylmalonate (20 mL, 130 mmol) was heated to 200 °C for 3.5 h.[14] The heat was then removed and the diethylmalonate was removed under a stream of argon as the reaction was allowed to cool to rt. The solid product was purified by chromatography on silica gel twice (50% EtOAc/hexanes, followed by 5% MeOH/CH_2Cl_2) to yield 1.7 g (12.7%) of a yellow solid. ^{1}H NMR (400 MHz, DMSO-d_6) δ 11.71 (1H, br), 8.69 (1H, s), 8.25 (1H, s), 5.46 (1H, s), 2.30 (3H, s); HR-EI MS $(M)^+$ m/z calcd for $C_9H_7BrN_2O_2$ 253.9691, found 253.9674.

4.5.6. 9-Bromo-7-methyl-2-morpholin-4-yl-pyrido(1,2-a)-pyrimidin-4-one (TGX66). A stirred solution of **3** (1.7 g, 6.7 mmol) in $POCl_3$ (20.0 mL, 215 mmol) was heated to reflux overnight.[14] After 18 h, the reaction was quenched by pouring onto ice. The aqueous phase was extracted three times with CH_2Cl_2, concentrated to dryness in vacuo, and dissolved in EtOH (25 mL). Morpholine (1.5 mL, 17 mmol) was added to this solution and the reaction was heated to reflux for 1 h. After 1 h, the reaction was allowed to cool to rt, yielding a white precipitate. The precipitate was collected by filtration and rinsed with cold EtOH to yield 737 mg (38.8%) of a white solid. ^{1}H NMR (400 MHz, DMSO-d_6) δ 8.56 (1H, s), 8.14 (1H, s), 5.57 (1H, s), 3.63 (4H, s), 3.60 (4H, s), 2.26 (3H, s); ^{13}C NMR (100 MHz, $CDCl_3$) 160.6, 159.0, 142.4, 125.2, 122.3, 119.2, 118.9, 81.1, 65.8, 65.7, 44.8, 44.7, 18.0; HR-EI MS $(M)^+$ m/z calcd for $C_{13}H_{14}BrN_3O_2$ 323.0269, found 323.0259.

4.5.7. 9-Benzylamino-7-methyl-2-morpholin-4-yl-pyrido-(1,2-a)pyrimidin-4-one (TGX126). A stirred solution of TGX66 (15 mg, 0.046 mmol), $PdCl_2$ (dppf) (1.9 mg, 0.0023 mmol), potassium *tert*-butoxide (10.4 mg, 0.0928 mmol), and benzylamine (4.97 mg, 0.0464) in THF (1 mL) was heated to reflux for 24 h.[14] The product was purified by chromatography on silica gel (5% MeOH/CH_2Cl_2), followed by RP-HPLC, to yield 10 mg (61%) of a white solid. ^{1}H NMR (400 MHz, $CDCl_3$) δ 8.10 (1H, s), 7.22–7.31 (m), 6.35 (1H, s), 5.73 (1H, s), 4.47 (2H, s), 3.78 (4H, t, J = 4 Hz), 3.59 (4H, t, J = 4 Hz), 2.22 (3H, s); HR-EI MS $(M)^+$ m/z calcd for $C_{20}H_{22}N_4O_2$ 350.1743, found 350.1749.

4.5.8. 9-(3-Amino-phenyl)-7-methyl-2-morpholin-4-yl-pyrido[1,2-a]pyrimidin-4-one (MCA49). Prepared following the general procedure for TGX126, using TGX66 (50 mg, 0.16 mmol), 3-aminophenylboronic acid (96 mg, 0.62 mmol), and Na_2CO_3 (164 mg, 1.55 mmol) in place of potassium *tert*-butoxide. The product was purified by chromatography on silica gel (5% MeOH/EtOAc) to yield 30 mg (58%) of a white solid. LR-ESI MS $(M+H)^+$ m/z calcd for $C_{20}H_{22}N_4O_3$ 337.2, found 337.0.

4.5.9. 9-(2-Methoxy-phenylamino)-7-methyl-2-morpholin-4-yl-pyrido(1,2-a)pyrimidin-4-one (MCA50). Prepared following the general procedure for TGX126, using TGX66 (50 mg, 0.16 mmol) and *o*-anisidine (0.017 mL, 0.155 mmol). The product was purified by chromatography on silica gel (2% MeOH/hexanes) followed by RP-HPLC to yield 3.8 mg (6.7%) of a white solid. ^{1}H NMR (400 MHz, DMSO-d_6) δ 8.37 (1H, s), 8.04 (1H, s), 7.52 (1H, d, J = 8 Hz), 7.17 (1H, s), 6.98–7.09 (4H, m), 3.83 (3H, s), 3.70 (4H, t, J = 4 Hz), 3.62 (4H, t, J = 4 Hz), 2.23 (3H, s); HR-EI MS $(M)^+$ m/z calcd for $C_{20}H_{22}N_4O_3$ 366.1692, found 366.1701.

4.5.10. 7-Methyl-2-morpholin-4-yl-9-o-tolylamino-pyrido(1,2-a)pyrimidin-4-one (MCA51). Prepared following the general procedure for TGX126, using TGX66 (50 mg, 0.16 mmol) and *o*-toluidine (0.017 mL, 0.16 mmol). The product was purified by chromatography on silica gel (2% MeOH/hexanes) followed by RP-HPLC to yield 6.8 mg (12.6%) of an off-white solid. ^{1}H NMR (400 MHz, DMSO-d_6) δ 7.99 (1H, s), 7.82 (1H, s), 7.23–7.34 (3H, m), 7.12 (1H, t, J = 7.2 Hz), 6.48 (1H, s), 5.59 (1H, s), 3.64 (8H, br), 2.18 (3H, s), 2.15 (3H, s); HR-EI MS $(M)^+$ m/z calcd for $C_{20}H_{22}N_4O_2$ 350.1743, found 350.1754.

4.5.11. 9-(3,4-Dimethyl-phenylamino)-7-methyl-2-morpholin-4-yl-pyrido(1,2-a)pyrimidin-4-one (MCA52). Prepared following the general procedure for TGX126, using TGX66 (50 mg, 0.16 mmol) and 3,4-dimethylaniline (18.8 mg, 0.155 mmol). The product was purified by chromatography on silica gel (2% MeOH/hexanes) followed by RP-HPLC to yield 13.4 mg (23.9%) of a yellow solid. ^{1}H NMR (400 MHz, DMSO-d_6) δ 8.00 (1H, s), 7.85 (1H, br), 7.05–7.13 (3H, m), 6.94 (1H, s), 5.58 (1H, s), 3.64 (8H, br), 2.18–2.21 (9H, m); HR-EI MS $(M)^+$ m/z calcd for $C_{21}H_{24}N_4O_2$ 364.1899, found 364.1909.

4.5.12. 7-Methyl-9-(3-methyl-benzylamino)-2-morpholin-4-yl-pyrido(1,2-a)pyrimidin-4-one (MCA53). Prepared following the general procedure for TGX126, using TGX66 (50 mg, 0.16 mmol) and 3-methylbenzylamine (0.019 mL, 0.16 mmol). The product was purified by chromatography on silica gel (2% MeOH/hexanes) followed by RP-HPLC to yield 12.3 mg (22%) of an off-white solid. ^{1}H NMR (400 MHz, DMSO-d_6) δ 7.85 (1H, s), 7.09–7.19 (3H, m), 7.01 (1H, d, J = 8 Hz), 6.92 (1H, br), 6.32 (1H, s), 5.54 (1H, s), 4.43 (2H, s), 3.65 (4H, t, J = 5 Hz), 3.61 (4H, t, J = 5 Hz), 2.25 (3H, s), 2.11 (3H, s); HR-EI MS $(M)^+$ m/z calcd for $C_{21}H_{24}N_4O_2$ 364.1899, found 364.1904.

4.5.13. 9-(2,3-Dimethyl-phenylamino)-7-methyl-2-morpholin-4-yl-pyrido(1,2-a)pyrimidin-4-one (MCA54). Prepared following the general procedure for TGX126, using TGX66 (50 mg, 0.16 mmol) and 2,3-dimethylaniline (19 mg, 0.16 mmol). The product was purified by chromatography on silica gel (2% MeOH/hexanes) followed by RP-HPLC to yield 12.3 mg (22%). ^{1}H NMR (400 MHz, DMSO-d_6) δ 7.96 (1H, s), 7.83 (1H, s), 7.05–7.14 (3H, m), 6.30 (1H, s), 5.58 (1H, s), 3.64 (8H, br), 2.27 (3H, s), 2.13 (3H, s), 2.06 (3H, s); HR-EI MS $(M)^+$ m/z calcd for $C_{21}H_{24}N_4O_2$ 364.1899, found 364.1910.

4.5.14. 7-Methyl-9-(2-methyl-benzylamino)-2-morpholin-4-yl-pyrido(1,2-a)pyrimidin-4-one (MCA55). Prepared following the general procedure for TGX126, using TGX66 (50 mg, 0.16 mmol) and 2-methylbenzylamine (0.019 mL, 0.16 mmol). The product was purified by chromatography on silica gel (2% MeOH/hexanes) followed by RP-HPLC to yield 12.9 mg (23%) of an off-white solid. ^{1}H NMR (400 MHz, DMSO-d_6) δ 7.87 (1H, s), 7.09–7.17 (4H, m), 6.76 (1H, br), 6.31 (1H, s), 5.55 (1H, s), 4.44 (2H, s), 3.64 (4H, t, J = 5 Hz), 3.60 (4H, t, J = 5 Hz), 2.32 (3H, s), 2.11 (3H, s); HR-EI MS $(M)^+$ m/z calcd for $C_{21}H_{24}N_4O_2$ 364.1899, found 364.1905.

4.5.15. 5-Morpholin-4-yl-2-nitro-phenylamine (AMA30). Morpholine (2.03 mL, 23.2 mmol) was added to a stirred solution of 5-chloro-2-nitroaniline (2.0 g, 12 mmol) in DMSO (10 mL) and heated to 90 °C for 18 h.[23] When the reaction was complete, the product was precipitated by pouring into H_2O (150 mL), and then purified by chromatography on silica gel (50% EtOAc/hexanes) to yield 660 mg (25.4%) of a yellow solid. ^{1}H NMR (400 MHz, DMSO-d_6) δ 7.79 (1H, d, J = 8 Hz), 7.25 (2H, s), 6.34 (1H, d, J = 10 Hz), 6.18 (1H, s), 3.67 (4H, t, J = 5 Hz), 3.23 (4H, t, J = 5 Hz); ^{13}C NMR (100 MHz, DMSO-d_6) δ 155.9, 148.9, 127.8, 123.9, 105.8, 98.3, 66.4, 44.1; HR-EI MS $(M)^+$ m/z calcd for $C_{10}H_{13}N_3O_3$ 223.0957, found 223.0954.

4.5.16. 2-Hydroxy-4-morpholin-4-yl-benzaldehyde (IC60-211). DMF (10 mL) was cooled on ice and $POCl_3$ (1.4 mL, 15 mmol) was added dropwise. 3-Morpholinophenol (2.5 g, 14 mmol) was slowly added to the stirred solution at rt, incubated at rt for an additional 40 min, and then heated to 100 °C for 9 h essentially as described.[23] The reaction was terminated by dumping into 1 M NaOAc (40 mL). The solid was filtered, rinsed three times with H_2O, and purified by chromatography on silica gel (25% EtOAc/hexanes) to yield 802 mg (28%) of an off-white solid. ^{1}H NMR (400 MHz, DMSO-d_6) δ 11.07 (1H, s), 9.72 (1H, s), 7.46 (1H, d, J = 8 Hz), 6.55 (1H, dd, J = 9 Hz, 2.4 Hz), 6.28 (1H, d, J = 2.4 Hz), 3.66 (4H, t, J = 5 Hz), 3.30 (4H, t, J = 5 Hz); ^{13}C NMR (100 MHz, DMSO-d_6) δ 192.0, 163.7, 157.2, 133.9, 113.8, 106.8, 99.5, 66.4, 47.1; HR-EI MS $(M)^+$ m/z calcd for $C_{11}H_{13}NO_3$ 207.0895, found 207.0893.

4.5.17. 1-(2-Hydroxy-4-morpholin-4-yl-phenyl)-ethanone (IC86621). MeLi (2.4 mL of 1.6 M solution in Et_2O, 3.9 mmol) was added dropwise to a solution of IC60211 (200 mg, 0.996 mmol) in THF (4 mL) at −78 °C.[23] The reaction was allowed to warm to rt and proceed overnight, at which point the reagent was quenched with satd NH_4Cl (1 mL), extracted six times with Et_2O, and concentrated in vacuo. The product was chromatographed on silica gel (25% EtOAc/hexanes) to yield a white solid. The solid was dissolved in 10 mL MeCN, MnO_2 (391 mg, 4.5 mmol) was added, and the reaction was allowed to proceed for three days at rt under an inert atmosphere. The product was chromatographed on silica gel (50% EtOAc/hexanes) to yield 17.8 mg (18%) of a white solid. ^{1}H NMR (400 MHz, $CDCl_3$) δ 12.71 (1H, s), 7.55 (1H, d, J = 9 Hz), 6.35 (1H, d, J = 9 Hz), 6.26 (1H, s), 3.79 (4H, t, J = 5 Hz), 3.30 (4H, t, J = 5 Hz), 2.50 (3H, s); ^{13}C NMR (100 MHz, $CDCl_3$) δ 201.7, 165.0, 156.7, 132.5, 105.5, 100.6, 66.6, 47.2; HR-EI MS $(M)^+$ m/z calcd for $C_{12}H_{15}NO_3$ 221.1052, found 221.1049.

4.5.18. 1-(2-Hydroxy-4-morpholin-4-yl-phenyl)-phenyl-methanone (AMA37). Prepared according to the general procedure of IC86621 using PhMgBr (1.1 mL, 3.4 mmol) and IC60211 (150 mg, 0.724 mmol), except that the product of PhMgBr addition was taken on for oxidation by MnO_2 (249 mg, 3.38 mmol) without intervening chromatographic purification. Chromatography of the final product on silica gel (50% EtOAc/hexanes) yielded (28.9 mg, 14.1%) of a yellow solid. ^{1}H NMR (400 MHz, $CDCl_3$) δ 12.73 (1H, s), 7.41–7.61 (5H, m), 6.35 (1H, d, J = 2.4 Hz), 6.31 (1H, dd, J = 9 Hz, 2.8 Hz), 3.81 (4H, t, J = 8 Hz), 3.31(4H, t, J = 8 Hz); ^{13}C NMR (100 MHz, $CDCl_3$) δ 199.1, 166.1, 156.6, 138.8, 135.5, 131.4, 129.0, 128.4, 119.2, 111.3, 105.3, 100.6, 66.7, 47.1; HR-EI MS $(M)^+$ m/z calcd for $C_{17}H_{17}NO_3$ 283.1208, found 283.1195.

4.5.19. 2-Chloro-1-(2-hydroxy-4-morpholin-4-yl-phenyl)-ethanone (AMA48). A solution of 3-morpholinophenol (5.0 g, 28 mmol) and chloroacetonitrile (2.1 mL, 34 mmol) in chloroethane (150 mL) in a 3-neck flask was cooled in a ice bath, and BCl_3 (100 mL, 1 M in CH_2Cl_2) was slowly added by an addition funnel essentially as described.[23] $AlCl_3$ (1.9 g, 14 mmol) was then added to this solution, the flask was equipped with a reflux condenser, and the reaction was heated to 60 °C for 24 h. The reaction was then cooled to 0 °C and 100 mL 2 N HCl was added by addition funnel. Following acidification, the organic phase was collected and rinsed twice with 2 N HCl (100 mL) and once with H_2O (100 mL). The organic phase was concentrated in vacuo and the product purified by chromatography on silica gel (30% EtOAc/hexanes) to yield 775 mg (10.9%). ^1H NMR (400 MHz, DMSO-d_6) δ 11.91 (1H, s), 7.66 (1H, d, $J=9$ Hz), 6.53 (1H, dd, $J=9$ Hz, 2.4 Hz), 4.93 (2H, s), 3.66 (4H, t, $J=5$ Hz), 3.31 (4H, t, $J=5$ Hz); ^{13}C NMR (100 MHz, DMSO-d_6) δ 193.0, 163.6, 156.5, 132.1, 109.1, 105.8, 99.1, 65.7, 46.4, 46.3; HR-EI MS $(M)^+$ *m/z* calcd for $C_{12}H_{14}ClNO_3$ 255.0662, found 255.0670.

4.5.20. LY292223. Prepared according to the general procedure described for the synthesis of 2-aminochromones.[33] 2′-Hydroxyacetophenone (0.50 mL, 4.2 mmol) was dissolved in 11 mL CH_2Cl_2, cooled to −78 °C and $TiCl_4$ (6.5 mL, 1 M solution in THF, 6.5 mmol) was added. After 1 h, DIPEA (2.7 mL, 16 mmol) was added at −78 °C and the reaction was allowed to proceed for an additional 1 h. 4-Dichloromethylenemorpholin-4-ium[34] (1.2 g, 5.0 mmol) was then added and the reaction was allowed to proceed at −78 °C for 20 min. The reaction was warmed to 0 °C, MeOH (30 mL) was added, and the reaction was allowed to warm to rt overnight. The reaction was then concentrated in vacuo, washed once with satd $NaHCO_3$, and the $NaHCO_3$ was extracted three times with CH_2Cl_2. The combined organic phase was dried over $MgSO_4$, filtered, and solvent removed in vacuo. The product was purified by chromatography on silica gel (10% MeOH/EtOAc) to yield 344 mg of a white powder (36%). ^1H NMR (400 MHz, $CDCl_3$) δ 7.95 (1H, s), 7.35 (1H, s), 7.14 (1H, s), 7.08 (1H, s), 5.27 (1H, s), 3.63 (4H, t, $J=5$ Hz), 3.30 (4H, t, $J=5$ Hz); ^{13}C NMR (100 MHz, $CDCl_3$) δ 176.8, 162.5, 153.5, 132.2, 125.2, 124.6, 122.8, 116.3, 87.0, 65.8, 44.5; IR: 1616, 1555, 1418, 1300, 1251, 1117, 985, 766; HR-EI MS $(M)^+$ *m/z* calcd for $C_{13}H_{13}NO_3$ 231.0895, found 231.0887.

Acknowledgements

Z.A.K. is Howard Hughes Medical Institute Predoctoral Fellow, P.J.A. is a American Cancer Society Postdoctoral Fellow, and G.G.C. is a Kirschstein-NRSA Postdoctoral Fellow. We thank Dr. Jan Domin for cDNA encoding PI3KC2β, Dr. Tamas Balla for cDNA encoding PI4Kβ, and Dr. Tom Roberts for cDNA encoding p110β. This work was supported by NIH grants AI440099 (K.M.S.), CA52995 (R.T.A.), and an award to K.M.S. from the Sandler Program for Asthma Research. Mass spectra were provided by the Center for Mass Spectrometry at the University of California, San Francisco, supported by the NIH division of Research Resources.

Supplementary material

Supplementary data associated with this article can be found, in the online version, at doi:10.1016/j.bmc.2004.06.022.

References and notes

1. Katso, R.; Okkenhaug, K.; Ahmadi, K.; White, S.; Timms, J., et al. Cellular function of phosphoinositide 3-kinases: implications for development, homeostasis, and cancer. *Annu. Rev. Cell. Dev. Biol.* ***2000***, *17*, 615–675.
2. Anderson, K. E.; Jackson, S. P. Class I phosphoinositide 3-kinases. *Int. J. Biochem. Cell. Biol.* ***2003***, *35*, 1028–1033.
3. Arcaro, A.; Wymann, M. P. Wortmannin is a potent phosphatidylinositol 3-kinase inhibitor: the role of phosphatidylinositol 3,4,5-trisphosphate in neutrophil responses. *Biochem. J.* ***1993***, *296*(Pt 2), 297–301.
4. Wymann, M. P.; Bulgarelli-Leva, G.; Zvelebil, M. J.; Pirola, L.; Vanhaesebroeck, B., et al. Wortmannin inactivates phosphoinositide 3-kinase by covalent modification of Lys-802, a residue involved in the phosphate transfer reaction. *Mol. Cell. Biol.* ***1996***, *16*, 1722–1733.
5. Vlahos, C. J.; Matter, W. F.; Hui, K. Y.; Brown, R. F. A specific inhibitor of phosphatidylinositol 3-kinase, 2-(4-morpholinyl)-8-phenyl-4*H*-1-benzopyran-4-one (LY2940 02). *J. Biol. Chem.* ***1994***, *269*, 5241–5248.
6. Okkenhaug, K.; Bilancio, A.; Farjot, G.; Priddle, H.; Sancho, S., et al. Impaired B and T cell antigen receptor signaling in p110delta PI 3-kinase mutant mice. *Science* ***2002***, *297*, 1031–1034.
7. Jou, S. T.; Carpino, N.; Takahashi, Y.; Piekorz, R.; Chao, J. R., et al. Essential, nonredundant role for the phosphoinositide 3-kinase p110delta in signaling by the B-cell receptor complex. *Mol. Cell. Biol.* ***2002***, *22*, 8580–8591.
8. Sasaki, T.; Irie-Sasaki, J.; Jones, R. G.; Oliveira-dos-Santos, A. J.; Stanford, W. L., et al. Function of PI3Kgamma in thymocyte development, T cell activation, and neutrophil migration. *Science* ***2000***, *287*, 1040–1046.
9. Hirsch, E.; Katanaev, V. L.; Garlanda, C.; Azzolino, O.; Pirola, L., et al. Central role for G protein-coupled phosphoinositide 3-kinase gamma in inflammation. *Science* ***2000***, *287*, 1049–1053.
10. Vanhaesebroeck, B.; Jones, G. E.; Allen, W. E.; Zicha, D.; Hooshmand-Rad, R., et al. Distinct PI(3)Ks mediate mitogenic signalling and cell migration in macrophages. *Nat. Cell. Biol.* ***1999***, *1*, 69–71.
11. Ward, S. G.; Finan, P. Isoform-specific phosphoinositide 3-kinase inhibitors as therapeutic agents. *Curr. Opin. Pharmacol.* ***2003***, *3*, 426–434.
12. Ward, S.; Sotsios, Y.; Dowden, J.; Bruce, I.; Finan, P. Therapeutic potential of phosphoinositide 3-kinase inhibitors. *Chem. Biol.* ***2003***, *10*, 207–213.
13. Wymann, M. P.; Zvelebil, M.; Laffargue, M. Phosphoinositide 3-kinase signalling—which way to target? *Trends. Pharmacol. Sci.* ***2003***, *24*, 366–376.
14. Roberson, A.; Jackson, S.; Kenche, V.; Yaip, C.; Parbaharan, H.; Thompson, P. Therapeutic Morpholino-Substituted Compounds, WO 01/53266 A1, Thrombogenix, 2001.
15. Davies, S. P.; Reddy, H.; Caivano, M.; Cohen, P. Specificity and mechanism of action of some commonly

used protein kinase inhibitors *Biochem. J.* ***2000***, *351*, 95–105.
16. Walker, E. H.; Pacold, M. E.; Perisic, O.; Stephens, L.; Hawkins, P. T., et al. Structural determinants of phosphoinositide 3-kinase inhibition by wortmannin, LY294002, quercetin, myricetin, and staurosporine. *Mol. Cell.* ***2000***, *6*, 909–919.
17. Walker, E. H.; Perisic, O.; Ried, C.; Stephens, L.; Williams, R. L. Structural insights into phosphoinositide 3-kinase catalysis and signalling. *Nature* ***1999***, *402*, 313–320.
18. Zhao, X. H.; Bondeva, T.; Balla, T. Characterization of recombinant phosphatidylinositol 4-kinase beta reveals auto- and heterophosphorylation of the enzyme. *J. Biol. Chem.* ***2000***, *275*, 14642–14648.
19. Hall-Jackson, C. A.; Cross, D. A.; Morrice, N.; Smythe, C. ATR is a caffeine-sensitive, DNA-activated protein kinase with a substrate specificity distinct from DNA-PK. *Oncogene* ***1999***, *18*, 6707–6713.
20. Fukuchi, K.; Watanabe, H.; Tomoyasu, S.; Ichimura, S.; Tatsumi, K., et al. Phosphatidylinositol 3-kinase inhibitors, Wortmannin or LY294002, inhibited accumulation of p21 protein after gamma-irradiation by stabilization of the protein. *Biochim. Biophys. Acta* ***2000***, *1496*, 207–220.
21. Roshal, M.; Kim, B.; Zhu, Y.; Nghiem, P.; Planelles, V. Activation of the ATR-mediated DNA damage response by the HIV-1 viral protein R. *J. Biol. Chem.* ***2003***, *278*, 25879–25886.
22. Kashishian, A.; Douangpanya, H.; Clark, D.; Schlachter, S. T.; Eary, C. T., et al. DNA-dependent protein kinase inhibitors as drug candidates for the treatment of cancer. *Mol. Cancer Ther.* ***2003***, *2*, 1257–1264.
23. Halbrook, J.; Kesicki, E.; Burgess, L. E.; Schlachter, S. T.; Eary, C. T.; Schiro, J. S.; Huang, H.; Evans, M.; Han, Y. Materials and methods to potentiate cancer treatment, WO 02/20500 A2, ICOS Corporation, 2002.
24. Hollick, J. J.; Golding, B. T.; Hardcastle, I. R.; Martin, N.; Richardson, C., et al. 2,6-Disubstituted pyran-4-one and thiopyran-4-one inhibitors of DNA-dependent protein kinase (DNA-PK). *Bioorg. Med. Chem. Lett.* ***2003***, *13*, 3083–3086.
25. Sadhu, C.; Masinovsky, B.; Dick, K.; Sowell, C. G.; Staunton, D. E. Essential role of phosphoinositide 3-kinase delta in neutrophil directional movement. *J. Immunol.* ***2003***, *170*, 2647–2654.
26. Puri, K. D.; Doggett, T. A.; Douangpanya, J.; Hou, Y.; Tino, W. T., et al. Mechanisms and implications of phosphoinositide 3-kinase {delta} in promoting neutrophil trafficking into inflamed tissue. *Blood*, ***2004***.
27. Sadhu, C.; Dick, K.; Tino, W. T.; Staunton, D. E. Selective role of PI3K delta in neutrophil inflammatory responses. *Biochem. Biophys. Res. Commun.* ***2003***, *308*, 764–769.
28. Northcott, C. A.; Hayflick, J. S.; Watts, S. W. PI3-kinase upregulation and involvement in spontaneous tone in arteries from DOCA-salt rats: is p110delta the culprit?. *Hypertension* ***2004***, *43*, 885–890.
29. Sawyer, C.; Sturge, J.; Bennett, D. C.; O'Hare, M. J.; Allen, W. E., et al. Regulation of breast cancer cell chemotaxis by the phosphoinositide 3-kinase p110delta. *Cancer Res.* ***2003***, *63*, 1667–1675.
30. Kim, C. M.; Dion, S. B.; Onorato, J. J.; Benovic, J. L. Expression and characterization of two beta-adrenergic receptor kinase isoforms using the baculovirus expression system. *Receptor* ***1993***, *3*, 39–55.
31. Huang, X.; Chen, B. C. Synthesis of bisalkylthiolydine derivatives of meldrums acid and barbituric-acid. *Synthesis-Stuttgart*, ***1986***, 967–968.
32. Ye, F. C.; Chen, B. C.; Huang, X. Synthesis of 7-substituted 5-oxo-5h-thiazolo[3,2-*a*]pyrimidine-6-carboxylic acids, 2-substituted 4-oxo-4h-pyrido[1,2-*a*]pyrimidine-3-carboxylic acids, and 2,6-disubstituted 4-quinolones from meldrum acid-derivatives. *Synthesis-Stuttgart* ***1989***, *9*, 317–320.
33. Morris, J.; Luke, G. P.; Wishka, D. G. Reaction of phosgeniminium salts with enolates derived from Lewis acid complexes of 2′-hydroxypropiophenones and related beta-diketones. *J. Org. Chem.* ***1996***, *61*, 3218–3220.
34. Morris, J.; Wishka, D. G.; Fang, Y. A novel synthesis of 2-aminochromones via phosgeniminium salts. *J. Org. Chem.* ***1992***, *57*, 6502–6508.